AMSR-E/Aqua L2B Global Swath Surface Precipitation GSFC Profiling Algorithm, Version 4

USER GUIDE

How to Cite These Data

As a condition of using these data, you must include a citation:

Kummerow, C., R. Ferraro, and D. Randel. 2021. *AMSR-E/Aqua L2B Global Swath Surface Precipitation GSFC Profiling Algorithm, Version 4*. [Indicate subset used]. Boulder, Colorado USA. NASA National Snow and Ice Data Center Distributed Active Archive Center. https://doi.org/10.5067/IR85TKB5BLM3. [Date Accessed].

FOR QUESTIONS ABOUT THESE DATA, CONTACT NSIDC@NSIDC.ORG

FOR CURRENT INFORMATION, VISIT https://nsidc.org/data/AE_Rain

National Snow and Ice Data Center

TABLE OF CONTENTS

1 DATA DESCRIPTION

1.1 Parameters

This data set reports instantaneous surface precipitation rate and type over ice- and snow-free land and ocean, plus the integrated liquid and ice water content of the atmospheric column. Ancillary and QA data are also provided.

1.2 File Information

1.2.1 Format

Data are provided in Hierarchical Data Format - Earth Observing System, Version 5 (HDF-EOS5). HDF-EOS5 is a file format and software library that augments standard HDF5 with conventions, data types, and metadata elements specific to NASA EOS mission data.

1.2.2 File Contents

Within HDF-EOS5 data files, similar variables such as science data and file attributes are grouped together. As shown in Figure 1, AE_Rain Version 4 science data are stored in:

`/SWATHS/AMSRE_L2A/Data Fields/`

Latitude, longitude, and time data are stored in:

`/SWATHS/AMSRE_L2A/Geolocation Fields/`.

The `/HDFEOS INFORMATION/` subgroup contains HDF-EOS5 core and structural metadata.

The `npixs`, `nscans`, and `ntimes` 1D arrays contain no science data. They are placeholder variables (HDF dimension scales) that certain applications use to associate each data point's position in the data array with its corresponding location in the data space.

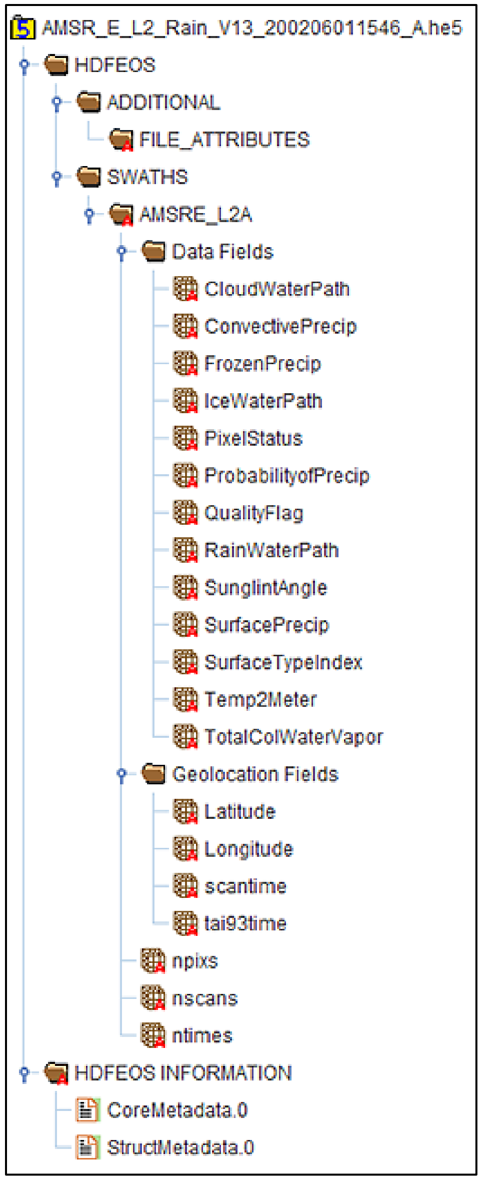

Figure 1. AE_Rain Version 4 Data Fields
(as seen in HDFView)

Table 1 contains names and descriptions for all the science data, geolocation, and temporal variables in AE_Rain Version 4 data files.

Table 1. Parameters and Descriptions

Parameter	**Description**	**Units**	**Fill**
CloudWaterPath	Total cloud liquid water in the atmospheric column.	kg/m^2	-9999.0
ConvectivePrecip	The instantaneous convective precipitation rate.	mm/hr	-9999.0
FrozenPrecip	The instantaneous frozen precipitation rate.	mm/hr	-9999.0
IceWaterPath	Total cloud ice in the atmospheric column.	kg/m^2	-9999.0

Parameter	Description	Units	Fill
PixelStatus	0: valid pixel 1: Invalid geolocation 2: Sensor Tb out of range 3: Surface code/histogram mismatch 4: Missing TCWV*, T2m**, or surface code 5: No Bayesian solution for pixel *Total column water vapor **2 m temperature	flag (0-5)	-99
ProbabilityofPrecip	Fraction of precipitation vs non-precipitation database profiles that make up the final solution.	percent	-99
QualityFlag	0: Good. Highest confidence of the best retrieval. 1: Use with caution. Can be set to 1 due to: sunglint present; RFI; geolocation, warm load, or other L1R warning flags. 2: Use with extreme care over snow-covered surface. Pixel is set to 2 if precipitation probability is poor quality or indeterminate. OK to use for climatological averaging of precipitation, but not for individual storm-scale daily cases. 3: Use with extreme caution. Pixels are set to 3 when the choice is made to retain the pixel despite missing channels that are critical for retrieval.	n/a	-99
RainWaterPath	Total rainwater in the atmospheric column.	kg/m^2	-9999.0
SunglintAngle	Relative angle of reflection between the sun and instrument line of sight.	degrees	-88
SurfacePrecip	Instantaneous total precipitation rate at the surface.	mm/hr	-9999.0
SurfaceTypeIndex	1: Ocean 2: Sea Ice 3:-7: Decreasing vegetation (3 = max, 7 = min) 8-11: Decreasing snow coverage (8 = max, 11 = min) 12: Inland water 13: Land/water boundary (coast) 14: Sea-Ice/ocean boundary	Index	-99
Temp2Meter	Temperature at 2 meters (K).	K	-999
TotalColWaterVapor	Integrated water vapor in the atmospheric column (TCWV); synonymous with Total Precipitable Water.	mm	-99
Latitude	Latitude of pixel center	degrees	-9999.0
Longitude	Longitude of pixel center	degrees	-9999.0
scantime	Scan start time along track in year, month, day, hour, minute and second	n/a	0

Parameter	Description	Units	Fill
tai93time	Scan time (International Atomic Time) in seconds from 01 January 1993 (TAI93)	seconds	-9999.0

1.2.3 Naming Convention

Example file name:

```
AMSR_E_L2_Rain_V13_200206011546_A.he5
AMSR_E_L2_Rain_[X][##]_[yyyy][mmdd][hhmm]_f.[ext]
```

Tables 2 and 3 describe the variables in the AE_Rain, Version 4 file naming convention.

Table 2. File Name Variable Descriptions

Variable	Description
X	Product maturity code (see Table 3)
##	File version number
yyyy	Four-digit year
mmdd	Two-digit month and day
hhmm	Hour and minute (UTC time) of first scan in file
f	Direction of travel (A = ascending, D = descending)
ext	File extension: .he5 (HDF-EOS) .jpg (browse image) .qa (quality assurance) .ph (product history) .xml (science metadata)

Table 3. Maturity Code Key

Maturity Codes	Description
P (preliminary)	Non-standard, near-real-time data. These data are only available until the corresponding standard product is ingested.
B (beta)	Developing algorithm with updates anticipated.
T (transitional)	Beyond beta, but not quite ready for validation.
V (validated)	Products are upgraded to validated once the algorithm has been verified by the algorithm team. Validated products have an associated validation stage (see).

1.3 Spatial Information

1.3.1 Coverage

Coverage includes all ice-free and snow-free land and ocean between 89°24' N and -89°24' S.

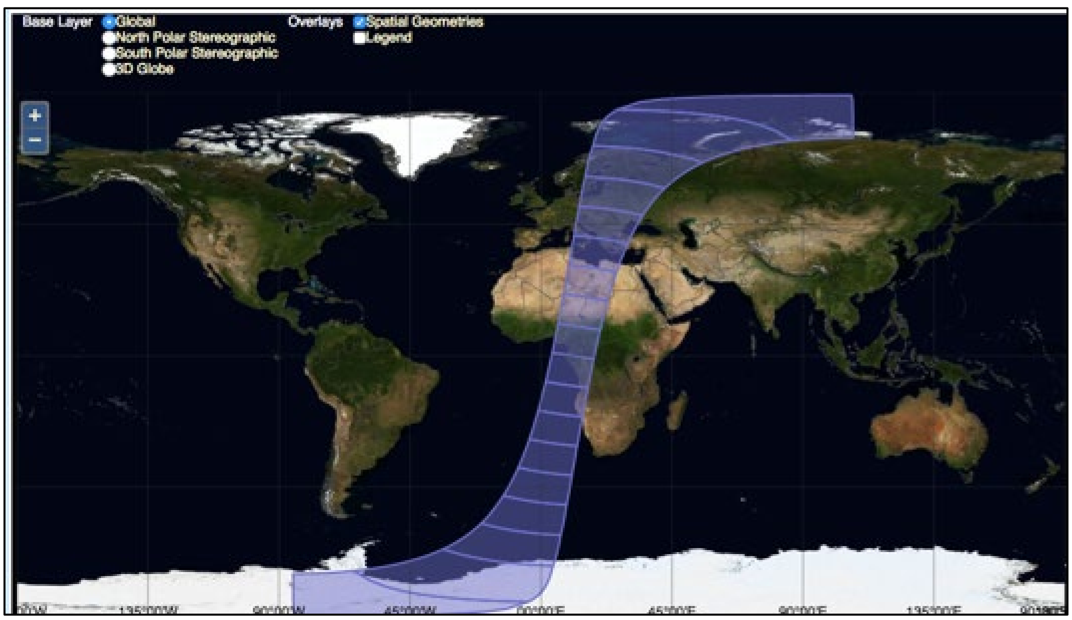

Figure 2. Swath coverage during one half orbit of the AMSR-E instrument.

1.3.2 Resolution

10 km (along track) by 5 km (along scan)

1.3.3 Geolocation

Data are provided with latitude and longitude.

1.4 Temporal Information

1.4.1 Coverage

1 June 2002 to 4 October 2011

1.4.2 Resolution

Each half-orbit swath spans approximately 50 minutes. The data sampling interval is 2.6 ms per sample for the 6.9 GHz to 36.5 GHz channels and 1.3 ms for the 89.0 GHz channel. A full scan takes approximately 1.5 seconds.

2 DATA ACQUISITION AND PROCESSING

The following sections reference the "Global Precipitation Measurement (GPM) Mission Algorithm Theoretical Basis Document" (ATBD for GPROF2017 Version 1).

2.1 Acquisition

This data set is generated from the following input data:

- AMSR-E/Aqua L2A Global Swath Spatially-Resampled Brightness Temperatures, Version 4 (AE_L2A, V4);
- An a priori database of observed cloud and precipitation profiles obtained by the Global Precipitation Measurement (GPM) mission;
- 2 m temperature, total column water vapor, and surface type data (included in data files).

The a priori database contains high resolution, vertical, precipitation distribution profiles and estimates of surface rainfall rates. Profiles over oceans are generated using the GPM Combined Radar-Radiometer Precipitation Algorithm (V5), which utilizes measurements from both the GPM Microwave Imager (GMI) and the Dual Frequency Precipitation Radar (DPR). Profiles over land and coastal regions are produced using the DPR Ku-band only and the DPR algorithm (V4). Additional information is provided in "Section 3.3 | The A-Priori Databases" in the ATBD for GPROF2017.

Surface type classifications are derived from: an emissivity-based scheme developed by Colorado State University (CSU) for the Special Sensor Microwave/Imager (SSM/I); a MODIS-SeaWIFS Ocean Color land mask; and the NOAA Autosnow daily fields (to identify areas of sea ice). Surface type classifications are discussed in more details in "Section 3.1.1 | Creating the Surface Class Specification" in the ATBD for GPROF2017.

2.2 Processing

GPROF 2017 utilizes a standard Bayesian inversion method to construct new hydrometeor profiles from an a priori database of previously observed profiles. In this approach, detailed in Kummerow et al. (1996), the probability of observing a particular rain profile R, for a given T_b, is written as:

$$Pr(R \mid T_b) = Pr(R) \times Pr(T_b \mid R),$$

where Pr(R) is the probability that a certain profile R will be observed and $Pr(T_b \mid R)$ is the probability of observing T_b given a particular rain profile R.

In practice, Pr(R) is derived from the a priori database of rain profiles and $Pr(T_b \mid R)$ is obtained by applying radiative transfer computations through the cloud model profiles. In brief, the inversion retrieves a modeled rain profile by computing the weighted sum of structures in the a priori database that are radiometrically consistent with input observations. The weighting scheme consists of an exponential factor computed as the mean square difference of the observed T_bs and a corresponding set of T_bs obtained from the radiative transfer calculations. The retrieval solution utilized by the algorithm is described in “Section 3.0 | Algorithm Description” of the ATBD for GPROF2017.

Users seeking a more detailed discussion of GPROF 2017’s implementation should consult sections 3.1–3.4 of the ATBD for GPROF2017, which address: ancillary data; how the algorithm resolves observations from different GPM radiometers with different spatial resolutions; ongoing changes to a priori database; and uncertainties associated with each channel in the Bayesian retrieval framework.

2.2.1 Precipitation Probability Threshold

For Version 4 of AE_Rain, GPROF 2017 applies a new rain/no-rain probability of precipitation (POP) threshold directly to retrieved precipitation values. In brief, the POP value represents the fraction of raining vs non-raining database profiles that make up the retrieved profile solution. POP thresholds are described in “Section 3.5 | Precipitation Probability Threshold” of the ATBD for GPROF 2017.

2.2.2 Precipitation Type

The rain profile retrieval process returns total surface precipitation, not the phase of the precipitation. To discriminate between liquid and frozen precipitation, GPROF 2017 uses lookup tables, one for ocean and one for land, that specify the fractional liquid precipitation for a range of dew point temperatures. At -6.5° C and below, all the precipitation is frozen; above 6.5° C, the precipitation is all liquid. Between these extremes, the precipitation is mixed. For additional details, see "Section 3.6 | Precipitation Type (Liquid vs. Frozen) Determination" of the ATBD for GPROF 2017.

2.3 Quality, Errors, and Limitations

2.3.1 Quality Assessment

Each HDF-EOS file contains core metadata with Quality Assessment (QA) metadata flags that are set by the Science Investigator-led Processing System (SIPS) at the Global Hydrology and Climate Center (GHCC) prior to delivery to NSIDC. A separate metadata file in XML format is also delivered to NSIDC with the HDF-EOS file; it contains the same information as the core metadata. Three levels of QA are conducted with the AMSR-E Level- 2 and -3 products: automatic, operational, and science QA. If a product does not fail QA, it is ready to be used for higher-level processing, browse generation, active science QA, archive, and distribution. If a granule fails QA, SIPS does not send the granule to NSIDC until it is reprocessed. Level-3 products that fail QA are never delivered to NSIDC (Conway 2002).

2.3.1.1 Automatic QA

Brightness temperatures are verified to be within physical bounds (50 K – 305 K) for all channels used by the rainfall algorithm. Automated QA for the rainfall algorithm is difficult because heavy rainfall can mask the surface, thereby hindering geo-location verification. As such, the rainfall algorithm relies on the Level 2A product to determine geolocation quality. As a final QA check on the computed rainfall, the brightness temperatures of the computed rainfall are compared with the observed brightness temperatures. If the difference between the two exceeds a pre-defined threshold, the rainfall is set to missing (PixelStatus=11).

The AMSR-E PixelStatus = 2 value is assigned when a brightness temperature is less than 40 or greater than 325, but the retrieval still runs with this pixel code. This is not related to the probability of precipitation. The probability of precipitation is determined from the Bayesian weighted probability of rain in the database, e.g., from the pixel's surface type, 2m temperature, and water vapor bin.

2.3.1.2 Operational QA

AMSR-E Level-2A data are subject to operational QA before they are used to generate higher-level products. Operational QA varies by product, but it typically checks the following criteria:

- File is correctly named and sized
- File contains all expected elements
- File is in the expected format

- Required EOS fields of Time, Latitude, and Longitude are present and populated
- Structural metadata are correct and complete
- The file is not a duplicate
- The HDF-EOS version number is provided in the global attributes
- The correct number of input files were available and processed

2.3.1.3 Science QA

In the Science Investigator-led Processing Systems (SIPS) environment, science QA includes verifying maximum and minimum values, percentage of missing data, and out-of-bounds data correspond with established tolerances. At the Science Computing Facility (SCF), as well as at GHCC, science QA involves reviewing the operational QA files, generating browse images, and performing the following additional automated QA procedures:

- Historical data comparisons
- Detection of errors in geolocation
- Verification of calibration data
- Trends in calibration data
- Detection of large scatter among data points that should be consistent

Geolocation errors are corrected during Level-2A processing to prevent processing anomalies such as extended execution times and large percentages of out-of-bounds data in downstream products. The Team Lead SIPS (TLSIPS) developed tools for use at SIPS and SCF for inspecting the data granules. These tools generate a QA browse image in Portable Network Graphics (PNG) format and a QA summary report in text format for each data granule. Each browse file shows Level-2A and Level-2B data. These are forwarded from the Remote Sensing Systems (RSS) to the GHCC along with associated granule information, where they are converted to HDF raster images prior to delivery to NSIDC. See AMSR-E Validation Data for information about the procedures and data used to check the accuracy and precision of AMSR-E observations.

2.3.2 Error Sources

Quantifying errors in this data set is complicated because it involves understanding the nature of precipitation. Uncertainties arise when the rain layer thickness is not well understood, or when inhomogeneous rainfall occurs below the resolution of the satellite. Another potential source of error is the non-precipitating component of clouds, which contribute to brightness temperatures. Scattering-based retrievals over land also present many uncertainties, most notably the lack of a consistent relationship between frozen rain aloft and liquid at lower altitudes. Quantifying the scattering by ice is especially problematic. Ambiguities occur in the data because microwave radiation is scattered not only by rainfall and associated ice, but by snow cover and dry land (Kummerow and Ferraro 2007).

In addition, sun glint can lead to missing precipitation rates. The sun glint angle, stored in the SunglintAngle variable, is the angular separation between the reflected satellite view vector and the sun vector. When this angle is zero, the instrument is viewing the center of the specular (mirror-like) sun reflection. If this angle is < 10°, the pixel is potentially affected by sun glint and its quality flag (QualityFlag) is lowered.

2.3.3 Limitations

- No profiles are retrieved over snow covered land surfaces. Suitable a priori profiles are currently unavailable.
- Light rain and drizzle in the high latitude are still poorly observed. Although GPROF 2017 increases precipitation at high latitudes over ocean, these values are probably still too low.
- Precipitation phase at high elevations is often incorrect (frozen precipitation is reported as rain). The crude resolution (often 50 km) of 2 m wet bulb temperatures cannot accurately capture low mountain temperatures.
- Precipitation in coastal regions remains lower in quality. When the satellite pixel encompasses both land and water in the field-of-view (coast surface class), the microwave surface emissivity depends greatly on the relative percentages of each.

For additional details, see “Section 5.0 | Known Limitations” in the ATBD for GPROF2017.

2.4 Instrument Description

See AMSR-E Instrument Description.

3 SOFTWARE AND TOOLS

For a list of tools that work with AMSR-E data, see the AMSR-E project page.

4 VERSION HISTORY

AE_Rain Version 4 data are generated from AMSR-E/Aqua L2A Global Swath Spatially-Resampled Brightness Temperatures, Version 4 (AE_L2A, V4) and GPROF 2017. See “AMSR-E Data Versions” for a summary of changes since the start of the mission.

5 CONTACTS AND ACKNOWLEDGMENTS

Christian Kummerow

Department of Atmospheric Science

Colorado State University

Fort Collins, CO

Paula Brown

Department of Atmospheric Science

Colorado State University

Fort Collins, CO

Ralph Ferraro

Earth System Science Interdisciplinary Center

University of Maryland

College Park, MD

David Randel

Department of Atmospheric Science

Colorado State University

Fort Collins, CO

6 REFERENCES

Conway, D. 2002. Advanced Microwave Scanning Radiometer - EOS Quality Assurance Plan. Huntsville, AL: Global Hydrology and Climate Center.

Elsaesser, G.S., and C.D. Kummerow. 2008. Toward a fully parametric retrieval of the nonraining parameters over the global oceans. Journal of Applied Meteorology and Climatology 47: 1599-1618.

Ferraro, R. R. 1997. SSM/I Derived Global Rainfall Estimates for Climatological Applications. Journal of Geophysical Research 102: 16,715-16,735.

Ferraro, R. R., and G. F. Marks. 1995. The Development of SSM/I Rain Rate Retrieval Algorithms Using Ground Based Radar Measurements. Journal of Atmospheric and Oceanic Technology 12: 755-770.

Grody, N. C. 1991. Classification of Snow Cover and Precipitation Using the Special Sensor/Microwave Imager (SSM/I). Journal of Geophysical Research 96: 7423-7435.

Kummerow, C., R. Ferraro, and David Randell. 2014. EOS/AMSR Rainfall: Algorithm Theoretical Basis Document, Version 2 GPROF 2010 L2A. Fort Collins, Colorado, USA: Colorado State University.

Kummerow, C., Y. Hong, W. S. Olson, S. Yang, R. F. Adler, J. McCollum, R. Ferraro, G. Petty, D. B. Shin, and T. T. Wilheit. 2001. The Evolution of the Goddard Profiling Algorithm (GPROF) for Rainfall Estimation from Passive Microwave Sensors. Journal of Applied Meteorology 40: 1801-1820.

Kummerow, C. D., S. Ringerud, J. Crook, D. Randel and W. Berg, 2010. An observationally generated a priori database for microwave rainfall retrievals, Journal of Atmospheric and Oceanic Technology 28(2): 113-130, doi: 10.1175/2010JTECHA1468.1.USER GUIDE: AMSR-E/Aqua L2B Global Swath Surface Precipitation GSFC Profiling Algorithm, Version 3

Kummerow, C., and R. Ferraro. 2006. [Supplement] EOS/AMSR-E Level-2 Rainfall: Algorithm Theoretical Basis Document. Fort Collins, Colorado, USA: Colorado State University. (PDF file, 245 KB)

Kummerow, C., and R. Ferraro. 2012. [Supplement] Algorithm Theoretical Basis Document: EOS/AMSR-E Level-2 Rainfall. Fort Collins, Colorado, USA: Colorado State University. (PDF file, 87 KB)

Kummerow, C., W. Olson, and L. Giglio. 1996. The Evolution of the Goddard Profiling Algorithm (GPROF) for Rainfall Estimation from Passive Microwave Sensors. IEEE Transactions on Geosciences and Remote Sensing 34: 1213-1232.

McCollum, J., and R. Ferraro. 2003. Next Generation of NOAA/NESDIS TMI, SSM/I, and AMSR-E Microwave Land Rainfall Algorithms. Journal of Geophysical Research - Atmospheres 108(D8): art. no. 8382.

McCollum, J. R., A. Gruber, and M. B. Ba. 1999. Discrepancy between gauges and satellite estimates of rainfall in equatorial Africa. Journal Applied Meteorology 41: 1065-1080.

Reynolds, R.W., T.M. Smith, C. Liu, D.B. Chelton, K.S. Casey, and M.G. Schlax, 2006: Daily high-resolution-blended analyses for sea surface temperature. Journal of Climate 20: 5473- 5496.

Wilheit, T., C. Kummerow, and R. Ferraro. 2003. Rainfall algorithms for AMSR-E. IEEE Transactions on Geosciences and Remote Sensing 41(2): 204-214.

7 DOCUMENT INFORMATION

7.1 Publication Date

November 2021

7.2 Date Last Updated

November 2021